Computers and Concrete, *Vol. 27, No. 4 (2021) 305-317*
DOI: https://doi.org/10.12989/cac.2021.27.4.305

Bond strength prediction of spliced GFRP bars in concrete beams using soft computing methods

Saeed Farahi Shahri[a] and Seyed Roohollah Mousavi*

Civil Engineering Department, University of Sistan and Baluchestan, Daneshgah Street, Zahedan, Iran

(*Received January 29, 2020, Revised February 16, 2021, Accepted February 25, 2021*)

Abstract. The bond between the concrete and bar is a main factor affecting the performance of the reinforced concrete (RC) members, and since the steel corrosion reduces the bond strength, studying the bond behavior of concrete and GFRP bars is quite necessary. In this research, a database including 112 concrete beam test specimens reinforced with spliced GFRP bars in the splitting failure mode has been collected and used to estimate the concrete-GFRP bar bond strength. This paper aims to accurately estimate the bond strength of spliced GFRP bars in concrete beams by applying three soft computing models including multivariate adaptive regression spline (MARS), Kriging, and M5 model tree. Since the selection of regularization parameters greatly affects the fitting of MARS, Kriging, and M5 models, the regularization parameters have been so optimized as to maximize the training data convergence coefficient. Three hybrid model coupling soft computing methods and genetic algorithm is proposed to automatically perform the trial and error process for finding appropriate modeling regularization parameters. Results have shown that proposed models have significantly increased the prediction accuracy compared to previous models. The proposed MARS, Kriging, and M5 models have improved the convergence coefficient by about 65, 63 and 49%, respectively, compared to the best previous model.

Keywords: bond strength; spliced GFRP bars; concrete beams; soft computing methods; genetic algorithm

1. Introduction

The bond between the bars and concrete is a key factor influencing the mechanical features of the structure (Turk *et al*. 2005, Ahmad *et al*. 2018, Golafshani *et al*. 2014) and an important design parameter that manages the performance of RC sections in both the ultimate and serviceability limit states (Lin *et al*. 2019). In different offensive environments, corrosion of steel reinforcement is one of the most momentous hazards found in reinforced concrete structures (Maurel *et al*. 2005, Yao *et al*. 2015, Moodi *et al*. 2017, Shirkhani *et al*. 2019). Corrosion of steel reinforcement leads to a large reduction of the effective cross-section of the steel rebars. As a result, the bond strength of rebar and concrete undergoes a notable decrease (Wang and Liu 2004). This has caused a growing need for such alternative materials as FRP bars for RC structures. GFRP bars have been more popular for their superior corrosion resistance, high strength-to-weight ratio, and high-cost efficiency (Nanni *et al*. 1995). For an optimum RC structure design, the load at the concrete and reinforcement interface should be transferred efficiently and reliably through the bond between the two materials (Golafshani *et al*. 2014). So far, numerous studies have been conducted to estimate the bar-concrete bond strength in spliced concrete beams. Ehsani *et al*. (1996) proposed a relationship to predict the bond strength of GFRP bars in terms of the bar diameter and concrete compressive strength. The Japanese Design Recommendation (1997) (JSCE) has predicted the bond strength of FRP bars in the splitting failure mode by modifying the steel bars' bond strength equation. Okelo and Yuan (2005) suggested a relationship similar to that of Ehsani *et al*. (1996) to estimate the bond strength of FRP bars. Considering the effects of bar diameter, splice length, concrete cover, and confinement provided by the transverse reinforcement, Aly (2005) predicted the bond strength of the GFRP and CFRP bars. Wambeke and Shield (2006) proposed a relationship to calculate the bond strength of GFRP bars through linear regressions on a database including RC beams with GFRP bars; the ACI 440.1R-15 guidelines (2015) has used their relationship. The CAN/CSA S806-12 code (2012) has determined the bond strength of FRP bars considering such parameters as the concrete cover, bar casting position, concrete strength, bar diameter, fiber type and bar surface properties. Choi *et al*. (2012) presented two relationships to predict the bond strength of the GFRP bars. Esfahani *et al*. (2013) predicted the bond strength of GFRP bars by the Monte Carlo simulation method considering the effects of such parameters as the transverse reinforcement, bar surface properties, bar diameter, and concrete compressive strength. The CAN/CSA-S6-14 (2014) has predicted the bond strength of FRP bars considering the effects of bar elasticity modulus, confinement, concrete cover, bar casting position, bar diameter, and bar surface properties. Xue *et al*. (2014) proposed a relationship to calculate the bond strength of the GFRP bars with diameters less than 20 mm and embedment

*Corresponding author, Associate Professor
E-mail: s.r.mousavi@eng.usb.ac.ir
[a]Ph.D. Student
E-mail: saeed_farahi@pgs.usb.ac.ir

ISSN: 1598-8198 (Print), 1598-818X (Online)

lengths less than 20 times the bar diameter. Using the artificial neural network and genetic programming approaches, Golafshani *et al*. (2015) predicted the bond strength of GFRP bars considering the effects of seven different variables. Ashrafi *et al*. (2017) proposed an empirical relationship to predict the ultimate tensile stress and the free-end slip of GFRP bars. Bazli *et al*. (2017) developed some equations to evaluate the influence of various parameters on the bond strength between the different types of concrete and GFRP bars under environmental conditions. Rakhshanimehr *et al*. (2018) suggested some equations for the local bond strength and displacement modulus of GFRP bars and finally presented a relationship for the bond strength of spliced GFRP bars in RC beams considering the non-uniform distribution of the bond stress along with the splice and effects of the elasticity modulus of the GFRP bars. Koroglu (2018) proposed ANN and regression models to forecast the FRP bar-concrete bond strength.

Although researches that estimate the bond strength of GFRP bars are numerous, studies have shown that the prediction accuracy of their proposed relationships can be improved. To this end, some researchers have suggested that different coefficients of existing relationships can be modified to enhance the prediction accuracy (Zemour *et al*. 2018). Some others have used machine learning and soft computing methods to achieve higher prediction accuracy (Golafshani *et al*. 2015). A reliable experimental database, including the 112 spliced concrete beams reinforced with GFRP bars, has been collected from the literature. Most previous models have estimated the bond strength much more or much less than the test values. This paper has made use of the improved MARS, Kriging, and M5 models to forecast the bond strength of GFRP bars in spliced concrete beams with high precision. Since proper selection of regularization parameters would greatly affect the fitting of the models, to enhance the prediction efficiency and accuracy, parameters effective in their fitting have been optimized by the genetic algorithm (GA). To ensure the generalization ability of the proposed models, training and testing data have been considered based on the ten-fold cross-validation technique. The results of the proposed methods have compared with those of other earlier researches and design codes.

2. Effective parameters in calculating the GFRP bar-concrete bond strength

2.1 Bar casting position

It was recognized that air bubbles and water move upward during the concrete casting and get stuck under the rebar. This occurrence reduces the linkage surface between bar and concrete and leads to a significant loss in the bond strength of top-cast bar specimens (Chaallal and Benmokrane 1993, Ehsani *et al*. 1993, Tighiouart *et al*. 1998). So far, several researchers have done some tests to determine the effects of top-cast GFRP bars on the concrete-bar bond strength. Chaallal and Benmokrane (1993) proposed a top bar factor of 1.23 for normal-strength and 1.18 for high-strength concrete. Ehsani *et al*. (1996) presented a 1.25 coefficient for the top bar effect. The JSCE (1997) used a 1.3 coefficient for the top-cast bar specimens. After testing the pullout specimens, and to consider the top bar factor of the GFRP bars, Tighiouart *et al*. (1998) suggested a 1.3 coefficient based on which the ACI 440.1R-03 guidelines (2003) considered the same coefficient for the top bar specimens. Wambeke and Shield (2006) proposed a 1.5 coefficient which was then used by ACI 440.1R-06 (2006) and ACI 440.1R-15 (2015). The CAN/CSA S806-12 (2012) and CAN/CSA S6-14 (2014) design recommendations advised a coefficient of 1.3 for the top-cast specimens. Pay *et al*. (2014) concluded that specimens with top bars experienced an average 7% loss in bond strength compared to those with bottom bars. Park *et al*. (2016) considered vertical, horizontal bottom, and horizontal top casting positions for the bar; results showed that the average bond strength of the horizontal bottom and horizontal top castings were, respectively, 91 and 40% of that of the vertical casting. Saleh *et al*. (2019) concluded that the bond strength of the specimens with bottom bars was more than that with top bars. To study this effect more precisely, the current paper has collected some similar-characteristic test specimens (Table 1), has found the bond strength ratio of specimens with bottom bars to those with top bars to be 1.12, and has divided the bond strength (estimated through soft computing models) by 1.12 for specimens with top GFRP bars.

2.2 Concrete compressive strength

Studies have revealed that the compressive strength of the concrete nearby the rebar is straightly relevant to the failure type as well as the bond strength. Malvar (1994) showed that for the splitting failure, an increment in the concrete compressive strength would improve the bond strength. Results of the studies of many researchers have shown that the bond strength of FRP bars and concrete has a good relevance with the square root of the concrete compressive strength (Faza and GangaRao 1990, Pleimann 1987, Okelo and Yuan 2005). Achillides and Pilakoutas (2004) found that for the high-strength concrete (>30 MPa), failure would appear on the surface of the FRP reinforcement, and when compressive strength was close to 15 MPa, the concrete damaged in front of the ribs of the FRP reinforcement. Lee *et al*. (2009) concluded that the bond strength of the steel and helically wrapped GFRP bars was more proportionate to the concrete compressive strength, and that of the sand-coated GFRP bars was determined more by the relative interfacial strengths of interfaces. Baena *et al*. (2009) showed that the concrete strength influenced the failure mode, and the bond strength of FRP reinforcement did not depend much on the concrete compressive strength for values of more than 30 MPa. Zhou *et al*. (2012) observed that an increment in the concrete strength would enhance the bond strength of the sand-coated GFRP bars. Hossain *et al*. (2017) studied the bond characteristics of GFRP bars in the high-strength concrete and ultra-high-strength concrete and concluded that bond

Table 1 Bond strength comparison for specimens with bottom and top-cast GFRP bars

References	Specimens	u_{bot}/u_{top}
Ehsani *et al*. (1996)	46B3Bl,46B3T1	1.25
	46B3B2,46B3T2	1.20
	46B6B2,46B6T2	1.22
	46B12B2,46B12T2	1.07
	86B12B2,86B12T2	1.03
	46B16B4,46B16T4	1.06
	86B16B4,86B16T4	1.04
	49B22B2,49B22T2	1.02
	89B22B2,89B22T2	1.04
	49B26B4,46B26T4	1.04
	89B26B4,89B26T4	1.04
	43PB,43PM	1.04
	43PB,43PT	1.05
	46PB,46PM	1.19
	46PB,46PT	1.24
	86PB,86PM	1.09
	86PB,86PT	1.13
	49PB,49PM	1.13
	49PB,49PT	1.15
	89PB,89PM	1.08
	89PB,89PT	1.10
Tighiouart *et al*. (1999)	12B,12T	1.26
	19B,19T	1.32
Pay *et al*. (2014)	B-HG-8-12b,B-HG-8-12b	1.04
	B-HG1-5-24b,B-HG1-5-24	1.08
	B-PG-5-24b,B-PG-5-24	1.06
	B-HG1-5-12b,B-HG1-5-12	1.27
	B-PG-5-12b,B-PG-5-12	1.28
	B-HG-8-24b,B-HG-8-24	1.11
Saleh *et al*. (2019)	A-9.5-5d-B,A-9.5-5d-T	1.04
	A-12.7-5d-B,A-12.7-5d-T	1.14
	A-15.9-5d-B,A-15.9-5d-T	1.15
	A-9.5-10d-B,A-9.5-10d-T	1.10
	A-12.7-10d-B,A-12.7-10d-T	1.01
	A-15.9-10d-B,A-15.9-10d-T	1.01
	B-9.5-5d-B,B-9.5-5d-T	1.02
	B-12.7-5d-B,B-12.7-5d-T	1.21
	B-15.9-5d-B,B-15.9-5d-T	1.40
	B-9.5-10d-B,B-9.5-10d-T	1.10
	B-12.7-10d-B,B-12.7-10d-T	1.09
Average		1.12
Standard deviation		0.09

strength would improve with increasing the concrete compressive strength.

2.3 Bar diameter

For an assumed splice length, the entire bond force generated by the bar increases with increasing the bar diameter. Since the increase rate of bond strength is less than that of the bar cross-sectional area, an increase in the bar diameter will reduce the bond stress. Using the bar with higher diameter leads to the reduction of pullout stress. Thus, as the bar diameter increases, a higher splice length is needed (Nanni *et al*. 1995, Tighiouart *et al*. 1998). When the diameter of the bar is larger, more leakage water gets stuck under the rebar which will decrease the bar-concrete linkage surface and the bond strength (Ehsani *et al*. 1996, Tighiouart *et al*. 1998, Hao *et al*. 2006, Baena *et al*. 2009).

2.4 Concrete cover

The concrete cover encloses the reinforcement and thus increases the bond strength. When the concrete cover is enough, splitting failure will be prevented or delayed (ACI 440.1R-03 2003). Ehsani *et al*. (1996) observed that the concrete cover extremely affected the bond failure type of GFRP bars. Aly (2005) showed that an increase in the concrete cover by up to four times the diameter of GFRP bars would increase the bond strength by 27%. Many papers have shown that the concrete cover thickness and bond strength of GFRP bars are related (Harajli and Abouniaj 2010, CAN/CSA S806-12 2012, Kotynia *et al*. 2017). The effect of the concrete cover has been regarded by the ratio of the concrete cover to the bar diameter (C/d_b). Where C is the minimum of the side cover, bottom cover, or one-half of the clear spacing between developed bars.

2.5 Splice or embedment length

An increase in the splice length will cause the bond stress distribution to be non-linearized and bond stresses to reduce; the more the splice length becomes, bond stresses will be distributed over a longer length thereby reducing the bar-concrete bond strength. Results of many studies have shown that an increase in the bar splice or embedment lengths will reduce the bond strength of GFRP bars (Achillides and Pilakoutas 2004, Okelo and Yuan 2005, CAN/CSA S806-12 2012, Saleh *et al*. 2019). Embedment length also affects the type of bond failure. Zhou *et al*. (2012) studied the bond behavior of sand-coated GFRP bars and showed that for embedment lengths less than five times the bar diameter, failure is of the pullout type, and for those more than that, it is of the splitting type. The effect of the splice length has been considered by the ratio of the splice length to the bar diameter (L/d_b).

2.6 Bar elasticity modulus

Achillides (1998) showed that the splitting bond strength of GFRP bars was close to 65 to 75% that of CFRP bars indicating the important role of the bar elasticity modulus in the splitting bond behavior. Mosley *et al*. (2008) conducted three sets of spliced beam tests with GFRP, AFRP, and steel bars and showed that the bond strength of FRP bars was much less than that of steel bars, and the bar elasticity modulus was a fundamental variable affecting the bond strength. Pay *et al*. (2014) also have pointed to the effect of the bar elasticity modulus on the bond strength. The effect of the bar elasticity modulus has been considered by the ratio of the elasticity modulus of steel bars to that of FRP bars (E_s/E_{frp}).

2.7 Bar surface properties

So far, many researchers have investigated the bond performance of various FRP bars with different surface features and shown that the presence of ribs on the bar surface would improve the bond behavior compared to non-ribbed surfaces. Makitani *et al*. (1993) concluded that surface features of FRP bars affect the bond strength. Although many researchers have pointed to the role of the bar surface features in the bond strength of FRP bars (Malvar 1994, Achillides and Pilakoutas 2004, Baena *et al*. 2009, Zhou *et al*. 2012, Esfahani *et al*. 2013), some others have believed that such features have had no significant effects on the bond strength (Wambeke and Shield 2006, Pay *et al*. 2014, Mosley *et al*. 2008). The parameter f_R accounts for the effect of bar surface properties based on the work by Esfahani *et al*. (2013).

2.8 Transverse reinforcement

So far, few researchers have examined the effects of transverse reinforcement on the bond strength of FRP bars; however, some have shown that its presence along the splice will prevent splitting cracks and will cause the bond force required for failure to increase (Orangun *et al*. 1977, Tepfers 1982). Achillides (1998) showed that in RC specimens with FRP bars, the transverse reinforcements restrict the crack width after the creation of the splitting cracks and, hence, improve the bond strength. Wambeke and Shield (2006) studied previous papers' test specimens with transverse reinforcements and concluded that their presence had no notable influence on the bond strength of GFRP bars may be due to their lower relative rib area. Some other researchers have pointed to the effects of transverse reinforcement on the enhancement of the bond strength (Kanakubo *et al*. 1993, Aly 2005, Esfahani *et al*. 2013). The effect of the transverse reinforcement has been considered by the ratio of the area of transverse reinforcement to the product of transverse reinforcement spacing, number of developed bars and bar diameter (A_t/snd_b).

3. Existing models in predicting bond strength of GFRP bars

The JSCE (1997) revised equations which were used to specify the bond strength for steel bars and proposed the following equation for FRP bars

$$u_m = f_{bod} / \alpha_1 \tag{1}$$

where u_m, f_{bod}, and α_1 are the bond strength of FRP bars, design bond strength of concrete, and confinement modification factor, respectively. The confinement modification factor can be determined by using the parameter k_c, as follows

$$k_c = \frac{C'}{d_b} + 15\frac{A_{tr}}{sd_b}\frac{E_{tr}}{E_s} \tag{2}$$

$$\begin{aligned} k_c \le 1.0 &\Rightarrow \alpha_1 = 1.0 \\ 1.0 \prec k_c \le 1.5 &\Rightarrow \alpha_1 = 0.9 \\ 1.5 \prec k_c \le 2.0 &\Rightarrow \alpha_1 = 0.8 \\ 2.0 \prec k_c \le 2.5 &\Rightarrow \alpha_1 = 0.7 \\ k_c \succ 2.5 &\Rightarrow \alpha_1 = 0.6 \end{aligned} \tag{3}$$

$$f_{bod} = \frac{0.28\alpha_2 \sqrt[3]{f_c'^2}}{1.3} \le 3.2 \, N/mm^2 \tag{4}$$

where C' is the minimum of bottom clear cover of main reinforcement and half of the clear space between the developed reinforcement (mm), d_b is the bar diameter (mm), A_{tr} is the area of transverse reinforcement (mm^2), s is the spacing between the transverse reinforcement (mm), E_{tr} is the elasticity modulus of transverse reinforcement (MPa), E_s is the elasticity modulus of steel (MPa), f_{bod} is the design bond strength between concrete and bar (MPa), α_2 is the modification factor for bond strength, and f'_c is the compressive strength of concrete (MPa).

Okelo and Yuan (2005) performed 151 pullout tests on FRP (AFRP, CFRP, and GFRP) and steel bars to investigate their bond characteristics. They presented the following equation to estimate the bond strength of FRP bars

$$u_m = \frac{14.7\sqrt{f_c'}}{d_b} \tag{5}$$

Aly (2005) tested 33 beam specimens reinforced with spliced carbon or glass FRP bars. He proposed an equation for calculating the bond strength of tensile lap-splice of FRP bars, as follows

$$\frac{u_m}{\sqrt{f_c'}} = \left(\frac{1}{4490} + \frac{C}{1800d_b} + \frac{d_b}{108L_s}\right)\sqrt{E_{frp}} + \frac{A_{tr} f_{yt}}{41.5sd_b} \tag{6}$$

in which L_s is the splice length (mm), E_{frp} is the elasticity modulus of FRP bar (MPa), and f_{yt} is the yield stress of transverse reinforcement (MPa).

Wambeke and Shield (2006) used a manner similar to that used by Orangun *et al*. (1977) and presented the following expression for predicting the average bond strength of GFRP bars in the splitting mode of failure

$$\frac{u_m}{0.083\sqrt{f_c'}} = \frac{1}{\alpha}\left(4 + 0.3\frac{C''}{d_b} + 100\frac{d_b}{L_s}\right) \tag{7}$$

where C'' is the minimum of the cover to the center of the bar, and one-half of the center-to-center spacing of the developed bars (mm), and α is the top bar factor which was recommended to be 1.5 and 1 for top and bottom bar specimens, respectively. ACI 440.1R-06 (2006) subscribed to the equation proposed by Wambeke and Shield (2006) for predicting the bond strength of FRP bars. This equation has also been used by ACI Committee 440 for inclusion in the latest version (ACI 440.1R-15 2015).

Based on the CAN/CSA-S806-12 (2012), the bond strength between FRP rebars and concrete can be calculated from Eq. (8).

$$u_m = \frac{d_{cs}\sqrt{f_c'}}{1.15(k_1k_2k_3k_4k_5)\pi d_b} \tag{8}$$

where d_{cs} represents minimum of the distance from the concrete surface to the center of the developed bars and two-thirds of the center-to-center distance of the developed bars (shall not be taken greater than 2.5 times bar diameter), k_1 denotes bar location factor (1.0 for bottom cast bars and 1.3 for top cast bars), k_2 represents concrete density factor (1.0 for normal density concrete, 1.2 for semi-low-density concrete, and 1.3 for low-density concrete), k_3 corresponds to rebar size factor (1.0 for A_b>300 mm^2 and 0.8 for A_b≤300 mm^2), k_4 denotes bar fiber factor (1.25 for AFRP bars and 1.0 for GFRP and CFRP bars), and k_5 represents bar surface factor (1.0 for surface roughened or sand coated or braided surfaces, 1.05 for spiral pattern surfaces or ribbed surfaces, 1.8 for indented surfaces).

The bond strength of FRP bars as per Canadian Highway Bridge Design Code CAN/CSA-S6-14 (2014) can be obtained from Eq. (9)

$$u_m = \frac{f_{cr}(d_{cs} + K_{tr}E_{frp}/E_s)}{0.45\pi d_b k_1 k_4} \tag{9}$$

in which f_{cr} is the cracking strength of concrete (MPa), and K_{tr} is the transverse reinforcement index given by $A_{tr}f_{yt}/10.5sn$.

Choi *et al*. (2012) proposed two following equations to predict the average bond strength of the GFRP bars

$$\frac{u_m}{\sqrt{f_c'}} = 0.037 + 0.151\frac{C}{d_b} + 7.719\frac{d_b}{L_s} \tag{10}$$

$$\frac{u_m}{\sqrt{f_c'}} = \left(0.1\frac{C_{\max}}{C_{\min}} + 0.9\right)\left(0.026 + 0.148\frac{C}{d_b} + 7.709\frac{d_b}{L_s}\right) \tag{11}$$

where C_{max} and C_{min} are the maximum and minimum of the bottom and side concrete covers, respectively.

Esfahani *et al*. (2013) suggested the following equation for predicting the bond strength of GFRP bars

$$\frac{u_m}{0.083\sqrt{f_c'}} = \frac{1}{\alpha}\left(2.36 + 0.177\frac{C''}{d_b} + 59\frac{d_b}{L_s} + f_R\frac{A_{tr}f_{yt}}{sd_b}\right) \tag{12}$$

where f_R is the surface factor of GFRP bar (0.03 for helical wrapped, 0.08 for grooved, 0.17 for sand coated, and 0.21 for ribbed surfaces).

Xue *et al*. (2014) introduced the following expression for estimating the bond strength of GFRP bars with the diameter less than 20 mm and the embedment length less than 20 times bar diameter

$$u_m = \alpha'\left(5.27f_t\right)\left(1.477 - 0.028d_b\right)\left[2.59\left(\frac{L_d}{d_b}\right)^{-0.62}\right] \tag{13}$$

in which α' represents the coefficient of the outer surface of GFRP bar (1 for sand-coated deformed, 0.64 for sand-coated ribbed, and 0.67 for fabric coated bars), and f_t denotes the specified tensile strength of concrete (MPa).

Rakhshanimehr *et al*. (2018) proposed some equations for calculating the local bond strength (Eq. (14)) and the displacement modulus of GFRP bars based on the results of the eccentric and concentric pullout tests. The non-uniform distribution of bond stress (Eq. (15)) and the elasticity modulus of GFRP bars were included in their investigation. The bond strength of spliced GFRP bars was estimated by using Eq. (16).

$$u_c = 2.7\frac{C/d_b + 0.5}{C/d_b + 3.6}\sqrt{f_c'} \tag{14}$$

$$M = Cosh(0.0022L_d\sqrt{\frac{E_s}{E_{frp}}}\sqrt{\frac{3f_c'}{d_b}}) \tag{15}$$

$$u_m = \frac{0.24}{\alpha}u_c\left(1 + \frac{1}{M}\right)\left(0.85 + 0.15\frac{C_{med}}{C}\right) \tag{16}$$

where u_c denotes the positional bond strength, M represents the parameter of the non-uniform distribution of bond stress. C and C_{med} are the minimum and median of bottom cover, side cover and one-half of the center-to-center spacing of the developed bars, respectively.

4. Data set and modeling methodology

The database of the spliced concrete beams reinforced with GFRP bars in the splitting failure mode contains 112 specimens tested by Achillides (1998), Tighiouart *et al*. (1999), Aly (2005), Mosley *et al*. (2008), Harajli and Abouniaj (2010), Choi *et al*. (2012), Esfahani *et al*. (2013), Pay *et al*. (2014), Choi *et al*. (2014), Rezaei (2017), and Zemour *et al*. (2018). To avoid over-fitting errors and to ensure the generalization capability of proposed methods, the models are trained and tested according to the ten-fold cross-validation technique. In this technique, the database is randomly broken into ten divisions. Then, one of the divisions is selected to test the model, and the remaining divisions are used to train the model. This manner repeated ten times with different test divisions. To estimate the bond strength of GFRP bars, the effects of seven variables are considered as inputs. Table 2 shows the details of the range of variations of the input and output parameters of the test specimens in the database.

Soft computing and machine learning techniques that are quite widespread have been widely used in engineering problems and have shown great performance (Güneyisi *et al*. 2016, Asteris *et al*. 2019). This paper has made use of the MARS, Kriging, and M5 models to forecast the bond strength of GFRP bars in spliced concrete beams. Since the

Table 2 Ranges of input and output parameters in the database

Parameters	Minimum	Maximum	Mean	Standard deviation
f'_c (MPa)	20	72	35.55	10.18
d_b (mm)	8.5	25.4	15.06	3.60
C/d_b	1	3	1.73	0.46
L/d_b	15	75	34.94	12.25
E_s/E_{frp}	3.5	5.68	4.76	0.61
f_R	0.03	0.21	0.13	0.07
A_t/snd_b	0	0.05	0.01	0.01
u_m (MPa)	1.06	6.73	3.04	1.20

model presented by soft computing methods depends on their regularization parameters, the effort has been made in this paper to optimize these parameters by the GA so that the convergence coefficient of the training data for the fitted model may reach its highest possible value. To this end, the following objective function has been minimized by the GA and the optimum effective values of the regularization parameters of the MARS, Kriging, and M5 models have been determined.

$$\min RRSQ = \frac{1}{R^2_{train}} \tag{17}$$

where R^2_{train} is the determination coefficient of training data.

4.1 Multivariate adaptive regression splines (MARS)

Firstly, Friedman (1991) presented the MARS model. It is a regression model commonly used to develop a nonlinear model between a specified dependent variable and the independent variables. As shown in Eq. (18), MARS produces a model from the weighted basis functions in two stages, including the forward stage and backward stage.

$$\hat{y} = a_0 + \sum_{i=1}^{M} a_i B_i(x) \tag{18}$$

in which $\hat{y}$, a_0, B_i, a_i, and M are the output parameter, constant term, ith basis function, coefficient of the ith basis function, and number of basis functions, respectively. The model chooses entire feasible basis functions and relevant knot sites in the forward stage, so a complicated model is created which would over-fit the trained data. In the backward stage, the excessive basis functions with the minimum participation to the model are eliminated by using the generalized cross-validation (GCV) criterion (Williams and Gomez 2016, Conoscenti *et al*. 2016) which is given by

$$GCV = \frac{1}{n} + \frac{\sum_{i=1}^{n}(y_i - \hat{y}_i)^2}{(1 - C(M)/n)^2} \tag{19}$$

where y_i represents the ith target value, $\hat{y}_i$ denotes the ith predicted value, n is the number of data, and $C(M)$ corresponds to the model complexity penalty factor which increases with increasing the number of basis functions. The MARS model has been implemented using the ARESLab toolbox (Jekabsons 2010a) in the MATLAB. Regularization parameters that affect the MARS model fitting include the *Max funcs*, *C*, *Cubic*, *Cubic fast level*, *Max interactions*, *Min span*, *End span*, *Allow linear*, and *Self interactions*. Where *Max funcs* denotes the maximum number of basis functions in the forward stage, *C* represents the Generalized Cross-Validation (GCV) penalty per knot, *Cubic* is the type of piecewise function (true for piecewise-cubic and false for piecewise-linear functions), *Cubic fast level* is the level of piecewise-cubic modelling (0 for cubic modelling in both forward and backward stages, 1 for cubic modelling in the backward stage, 2 for cubic modelling of the final model), *Max interactions* is the maximum degree of interactions between input variables, *Min span* is a minimum span that takes every *Min span*-th observation for knot placement (-1 for automatic mode, 0 or 1 for disablement of this feature, and values greater than 1 for tuning the span length), *End span* denotes a span that do not permit knots locating near to the ends of the data intervals (-1 for automatic mode, 0 for disablement of this feature, and values greater than 1 for tuning the span length), *Allow linear* represents a factor that permits variables entering basis functions linearly (0 for disagreement with linear variables, 1 for linear variables, and 2 for preferment of linear variable), and *Self interactions* denotes the maximum degree of self interactions for any input variables (Jekabsons 2010a). The regularization parameters are optimized by the GA and are given in Table 3.

Table 3 Optimized regularization parameters for fitting the best MARS model

Parameters	Optimum Value	Parameters	Optimum Value
Max funcs	40	Cubic fast level	1
C	1	Max interactions	2
Cubic	false	Min span	1
End span	-1	Allow linear	0
Self interactions	1		

The proposed MARS model with the optimal values of the parameters will be as follows

$$\begin{aligned}\hat{y} = {} & 3.51 + 639.07BF1 + 75.7BF2 - 25.58BF3 - 1.52BF4 \\ & - 1.88BF5 - 3.41BF6 - 0.007BF7 - 0.003BF8 + 3.81BF9 \\ & + 460.71BF10 + 34.52BF11 - 33.23BF12 - 1427.27BF13 \\ & - 100.73BF14 + 3.27BF15 - 38.54BF16 + 41.01BF17 \\ & + 1.21BF18 + 0.26BF19 + 0.05BF20 - 0.05BF21 - \\ & 0.15BF22 - 0.24BF23\end{aligned} \tag{20}$$

where *BF*s are basis functions which are given in Table 4. The proposed MARS model has yielded convergence coefficients equal to 0.97 and 0.88 for the training and testing data, respectively.

4.2 Kriging surrogate model

The main theorem of Kriging was offered by Krige (1951) and later expanded by Matheron (1970) and Sacks *et al*. (1989). Kriging is a stochastic regression model that employs the spatial covariance matrices to forecast the uncertain variables in new points (Al-Mudhafar 2019). The Kriging method can be defined as (Mallipeddi and Lee 2015, Li and Pan 2019)

$$\hat{y}(x) = \mu + Z(x) \tag{21}$$

in which $\hat{y}$ is the predicted value, μ is a regression parameter representing the average of the samples, and $Z(x)$ denotes a stochastic procedure with zero mean and covariance function as follows

$$\mathrm{COV}\left[Z(x^i), Z(x^j)\right] = \sigma_c^2 R\left[R(x^i, x^j, \theta)\right] \tag{22}$$

in Eq. (22), R defined as correlation matrix, σ_c^2 corresponds to the process variance, and θ is an uncertain correlation parameter to adjust the model. So, the Kriging

Table 4 Basis functions and corresponding equations of the MARS model

Basis Function	Equation
BF1	max(0,0.031-A_t/snd_b)
BF2	BF1*max(0,C/d_b-1.3)
BF3	max(0,C/d_b-1.309)*max(0,E_s/E_{frp}-5.585)
BF4	max(0,C/d_b-1.309)*max(0,5.585-E_s/E_{frp})
BF5	BF1*max(0,$f'c$-35.5)
BF6	BF1*max(0,35.5-f'_c)
BF7	max(0,54.016-L/d_b)*max(0,d_b-19.1)
BF8	max(0,54.016-L/d_b)*max(0,19.1-d_b)
BF9	max(0,54.016-L/d_b)*max(0,A_t/snd_b-0.026)
BF10	max(0,A_t/snd_b-0.031)*max(0,0.17-f_R)
BF11	BF1*max(0,L/d_b-33.333)
BF12	BF1*max(0,33.333-L/d_b)
BF13	max(0,0.028-A_t/snd_b)
BF14	BF13*max(0,4.260-E_s/E_{frp})
BF15	max(0,4.449-E_s/E_{frp})
BF16	BF13*max(0,L/d_b-50)
BF17	BF13*max(0,50-L/d_b)
BF18	max(0,12.7-d_b)
BF19	BF15*max(0,$f'c$-39)
BF20	max(0,E_s/E_{frp}-4.449)*max(0,36.3-f'_c)
BF21	BF18*max(0,L/d_b-20)
BF22	BF18*max(0,20-L/d_b)
BF23	BF15*max(0,f'_c-31)

model can be presented as

$$\hat{y}(x) = \hat{\mu} + r^T R^{-1}(y - 1\hat{\mu}) \tag{23}$$

here, $\hat{\mu}$ denotes the approximated regression parameter, r represents the correlation vector among the forecasted point and the entire known points, y corresponds to the vector comprising entire the samples. With assuming a value for θ, the approximated regression parameter $\hat{\mu}$ and the approximated variance $\widehat{\sigma_c^2}$ are determined using the following equations

$$\hat{\mu} = \frac{1^T R^{-1} y}{1^T R^{-1} 1} \tag{24}$$

$$\hat{\sigma}_c^2 = \frac{(y - 1\hat{\mu})^T R^{-1}(y - 1\hat{\mu})}{n} \tag{25}$$

To estimate θ, the following log-likelihood function should be maximized

$$Ln(\theta) = -\left[n \ln(\hat{\sigma}_c^2) + \ln|R| \right] / 2 \tag{26}$$

The Kriging model, that uses various correlation functions to control the model softness, has been implemented using the DACE toolbox (Lophaven *et al*. 2002) in the MATLAB Software. As shown in Table 5, the five regularization parameters (including the *Lower bound*, *Upper bound*, *Regrpply*, *CorrFunc*, and θ_0) effective in the Kriging model fitting have been optimized by the GA. *Lower bound*, *Upper bound*, and θ_0 respectively determine the minimum and maximum variation range of parameter θ and the initial θ guess. *Regrpply* and *CorrFunc* parameters specify the polynomial order and type of the correlation function (Exponential, Generalized exponential, Gaussian, Linear, Spherical, and Cubic spline), respectively. The model proposed by the Kriging method has yielded convergence coefficients of 0.99 and 0.85 for the training and testing data, respectively.

Table 5 Optimized regularization parameters for fitting the best Kriging model

Parameters	Optimum Value
Lower bound	0.4
Upper bound	2.4
Regrpply	1
CorrFunc	Linear
θ_0	0.4

Table 6 Optimized regularization parameters for fitting the best M5 model

Parameters	Optimum Value
Model tree	true
Min leaf size	3
Min parent size	6
Prune	false
Smoothing-K	5
Split threshold	0.3
Max depth	8

4.3 M5 model tree

Quinlan (1992) was the first researcher who proposed the M5 model tree and then this method expanded by Wang and Witten (1997). M5 is a data-driven model that changes the nonlinear relation of input and output variables into a piecewise linear relation. The M5 model is produced in two steps. First, the parameter space is divided into different subspaces and a linear regression function is built in every subspace. Thus, by employing the splitting criterion of the standard deviation reduction (SDR) factor, the main structure of the tree is built (Behnood *et al*. 2015, Mansouri *et al*. 2016, Nguyen *et al*. 2019)

$$SDR = sd(E) - \sum_i \frac{|E_i|}{|E|} sd(E_i) \tag{27}$$

where *sd* represents the standard deviation, E denotes the set of samples achieving the node, and E_i corresponds to the set of samples resulting from dividing the node. Second, the pruning step is executed to decrease the model complexity (Behnood *et al*. 2015, Mansouri *et al*. 2016). The M5 model has been implemented by the M5PrimeLab toolbox (Jekabsons 2010b) in the MATLAB environment. The seven regularization parameters (*Model tree*, *Min leaf size*, *Min parent size*, *Prune*, *Smoothing-K*, *Split threshold*, and *Max depth*) effective in the M5 model fitting have been optimized by the GA, as shown in Table 6. Where *Model tree* determines the type of tree (true for model tree and false for regression tree), *Min leaf size* is the minimum number of training samples for a leaf node, *Min parent size* is the minimum number of samples for dividing a node, *Prune* is the model pruning feature (true for model pruning

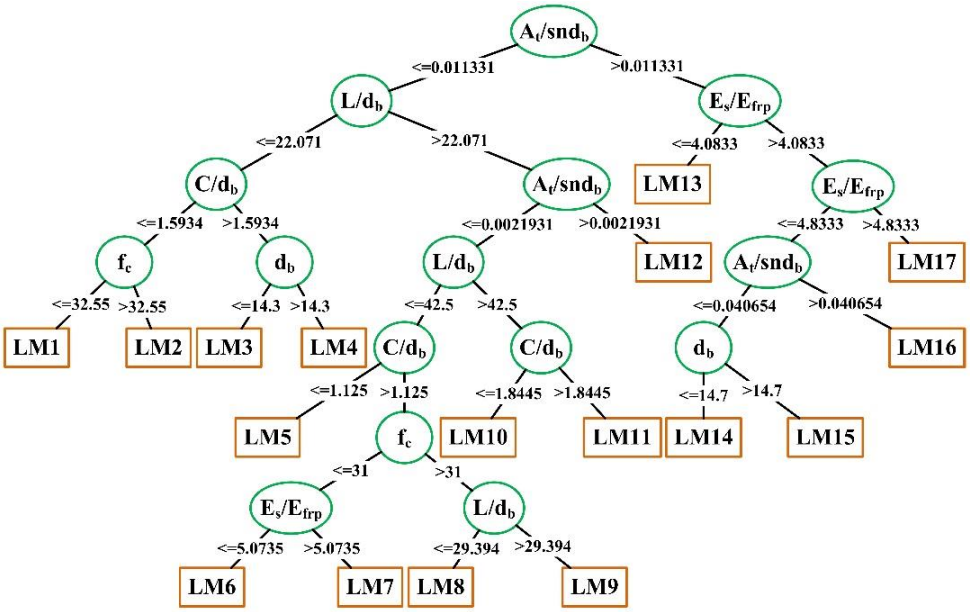

Fig. 1 proposed M5 structure for predicting the bond strength of spliced GFRP bars

and false for disabled model pruning), *Smoothing-K* is the smoothing parameter that softens sharp discontinuities, *Split threshold* is the minimum threshold for dividing the nodes of the tree, and *Max depth* is the maximum depth of a tree. The proposed M5 model has yielded convergence coefficients equal to 0.87 and 0.84 for the training and testing data, respectively.

The proposed M5 model tree with the optimal parameter is shown in Fig. 1 and the mathematical equations of each linear model (LM) are given in Table 7.

5. Comparison between proposed models and other existing models on bond strength of GFRP bars

To evaluate the accuracy of different models used in this research, the R^2, *AAE*, *RMSE*, and *MAE* statistical indices are employed, as follows

$$R^2 = 1 - \frac{\sum_{i=1}^{n}(y_{Expi} - y_{Predi})^2}{\sum_{i=1}^{n}(y_{Expi} - \bar{y}_{Exp})^2} \quad (28)$$

$$AAE = \frac{1}{n}\sum_{i=1}^{n}\frac{\left|y_{Exp,i} - y_{Pred,i}\right|}{y_{Exp,i}} \quad (29)$$

$$RMSE = \sqrt{\frac{\sum_{i=1}^{n}\left(y_{Exp,i} - y_{Pred,i}\right)^2}{n}} \quad (30)$$

$$MAE = \frac{1}{n}\sum_{i=1}^{n}\left|y_{Exp,i} - y_{Pred,i}\right| \quad (31)$$

where $\bar{y}_{Exp}$, $y_{Exp,i}$ and $y_{Pred,i}$ are the mean of the experimental responses, ith experimental and predicted responses, respectively. Fig. 2 shows the performance of different prediction models of the bond strength of spliced beams reinforced with GFRP bars. As shown, MARS and Kriging models, with correlation coefficients of respectively 0.94

Table 7 Equations of linear models of M5 model

No.	LM
1	y = 2.872 -0.005f'_c -0.004d_b +0.755C/d_b -0.016L/d_b -0.013E_s/E_{frp} +13.195A_t/snd_b
2	y = 2.811 -0.005f'_c -0.004d_b +0.755C/d_b -0.016L/d_b -0.013E_s/E_{frp} +13.195A_t/snd_b
3	y = 2.356 -0.003f'_c +0.045d_b +0.755C/d_b -0.016L/d_b -0.013E_s/E_{frp} +13.195A_t/snd_b
4	y = 2.458 -0.003f'_c +0.045d_b +0.755C/d_b -0.016L/d_b -0.013E_s/E_{frp} +13.195A_t/snd_b
5	y = 2.270 +0.004f'_c -0.005d_b +0.629C/d_b -0.025L/d_b -0.032E_s/E_{frp} +12.346A_t/snd_b
6	y = 3.719 -0.001f'_c -0.005d_b +0.466C/d_b -0.027L/d_b -0.142E_s/E_{frp} +12.346A_t/snd_b
7	y = 3.673 -0.001f'_c -0.005d_b +0.466C/d_b -0.027L/d_b -0.142E_s/E_{frp} +12.346A_t/snd_b
8	y = 3.037 -0.0004f'_c -0.005d_b +0.466C/d_b -0.032L/d_b -0.016E_s/E_{frp} +12.346A_t/snd_b
9	y = 2.949 -0.0005f'_c -0.005d_b +0.466C/d_b -0.031L/d_b -0.016E_s/E_{frp} +12.346A_t/snd_b
10	y = 1.863 +0.003f'_c -0.005d_b +0.482C/d_b -0.016L/d_b -0.028E_s/E_{frp} +12.346A_t/snd_b
11	y = 2.155 +0.003f'_c -0.005d_b +0.423C/d_b -0.016L/d_b -0.028E_s/E_{frp} +12.346A_t/snd_b
12	y = 3.056 +0.003f'_c -0.005d_b +0.365C/d_b -0.019L/d_b -0.037E_s/E_{frp} +29.911A_t/snd_b
13	y = 6.594 +0.004f'_c -0.068d_b +0.099C/d_b -0.010L/d_b -0.378E_s/E_{frp} +16.304A_t/snd_b
14	y = 4.477 +0.004f'_c -0.076d_b +0.099C/d_b -0.010L/d_b -0.035E_s/E_{frp} +19.295A_t/snd_b
15	y = 4.470 +0.004f'_c -0.077d_b +0.099C/d_b -0.010L/d_b -0.035E_s/E_{frp} +19.295A_t/snd_b
16	y = 4.489 +0.004f'_c -0.072d_b +0.099C/d_b -0.010L/d_b -0.035E_s/E_{frp} +20.058A_t/snd_b
17	y = 3.833 +0.004f'_c -0.076d_b +0.099C/d_b -0.010L/d_b +0.148E_s/E_{frp} +20.605A_t/snd_b

Table 8 Comparison of statistical indices for the proposed and existing models

Model	Average of $(u_m)_{Pred}/(u_m)_{Exp}$	Standard deviation of $(u_m)_{Pred}/(u_m)_{Exp}$	AAE	RMSE	MAE	R^2
JSCE (1997)	0.776	0.258	0.290	1.365	1.002	0.27
Aly (2005)	0.828	0.526	0.423	1.949	1.351	0.30
CAN/CSA S806-12 (2012)	1.486	0.591	0.581	1.717	1.447	0.08
Choi *et al*. (2012)	1.092	0.294	0.244	1.008	0.720	0.31
Esfahani *et al*. (2013)	0.843	0.200	0.209	0.994	0.697	0.57
CAN/CSA S6-14 (2014)	1.729	0.642	0.766	2.221	1.890	0.14
ACI 440.1R-15 (2015)	1.297	0.381	0.372	1.143	0.941	0.35
Rakhshanimehr *et al*. (2018)	0.916	0.284	0.246	1.121	0.807	0.37
M5	1.015	0.138	0.111	0.475	0.332	0.85
MARS	1.016	0.121	0.076	0.286	0.197	0.94
Kriging	1.009	0.102	0.048	0.318	0.142	0.93

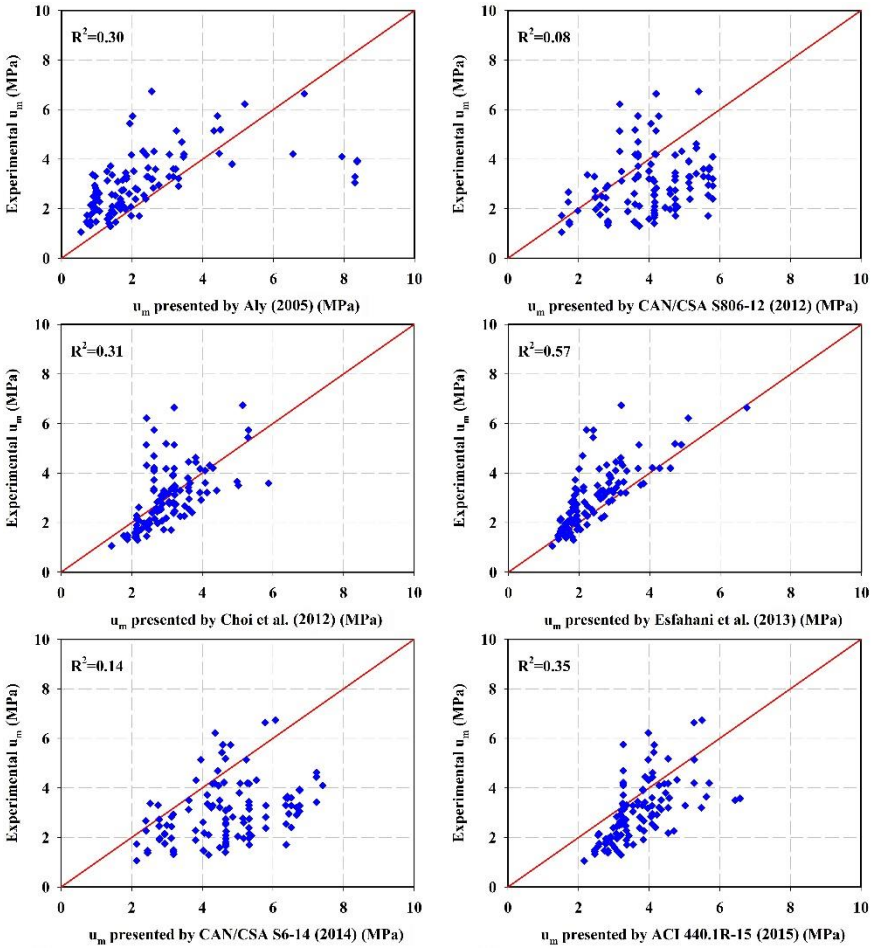

Fig. 2 Comparison of performance of different models for predicting the bond strength of spliced GFRP bars

and 0.93 have had the best performance, and M5 with correlation coefficient of 0.85 has provided better estimates compared to other existing models. Among the previous models, that of Esfahani *et al*. (2013) has provided a better estimate than other existing models (with a convergence coefficient of 0.57). The proposed MARS, Kriging, and M5 models have been able to nearly improve the convergence coefficient by 65, 63 and 49%, respectively, compared to that of Esfahani *et al*. (2013). The models provided by CAN/CSAS6-14 (2014) and CAN/CSA S806-12 (2012) have exhibited very low correlation coefficients (0.08 and 0.14, respectively).

Table 8 compares the accuracy and statistical indices of the proposed models with those of the existing ones. All 112 data samples were employed to compare the performance of different models. As shown, the proposed Kriging model has had the best value for the ratio of the predicted to experimental bond strengths and the lowest standard deviation compared to other models. The MARS and M5 models also have yielded a much better mean and standard deviation than other existing models. Among the previous models, the relationships presented by Esfahani *et al*.

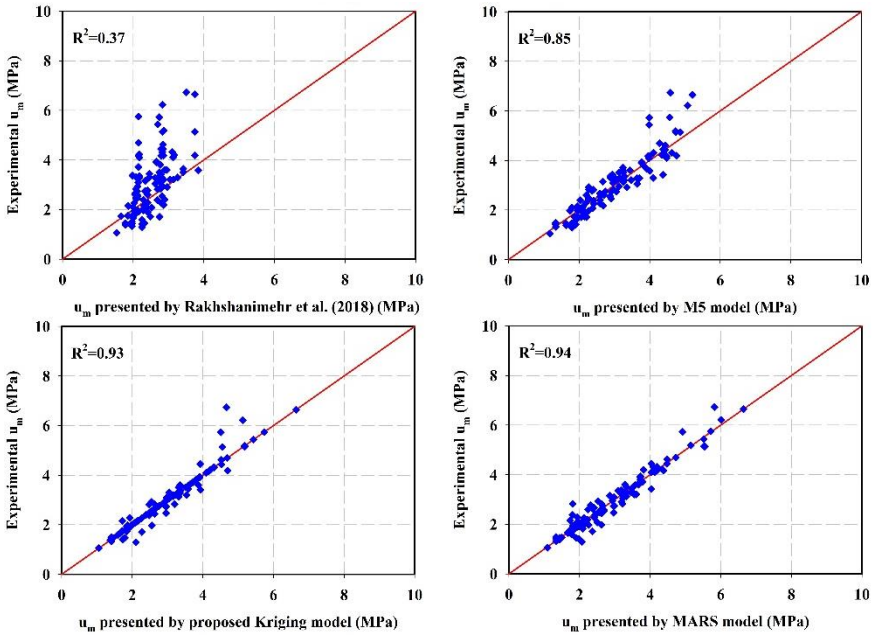

Fig. 2 Continued

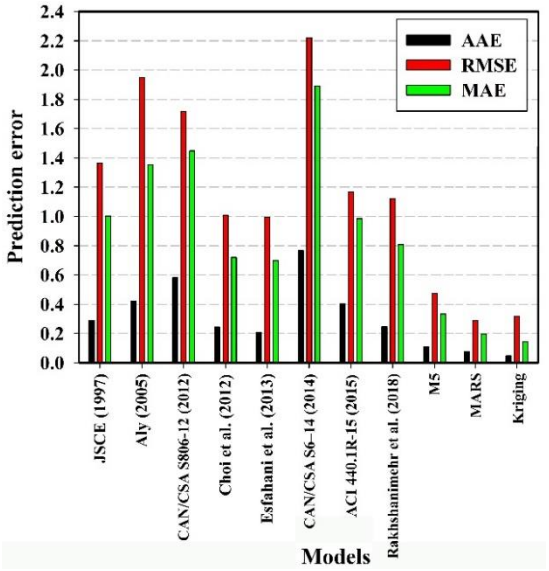

Fig. 3 Comparison of error indices for the proposed and existing models

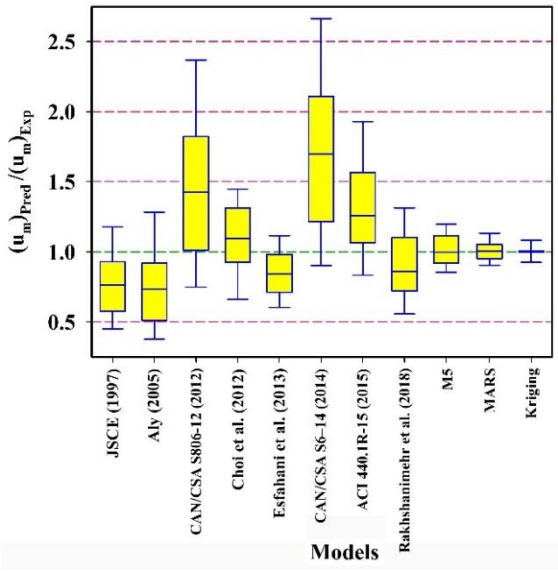

Fig. 4 Box plots of the ratio of the predicted to experimental bond strengths for different models

(2013), Choi *et al*. (2012), and Rakhshanimehr *et al*. (2018) have presented relatively better statistical indices than other ones. Regarding the RMSE statistical indicator, the MARS and then the Kriging model have had the least error while regarding AAE and MAE statistical indices, the Kriging and then the MARS model have presented a more accurate estimate than other models. The proposed MARS model has had the best convergence coefficient (R^2=0.94). It is worth noting that some previous models have been adapted from a smaller database and may be less accurate than the proposed models, which are based on a more extensive database.

The prediction errors of the proposed and previous models are compared in Fig. 3 where a comparison of the statistical indices of different models shows that the models presented by CAN/CSAS6-14 (2014), CAN/CSAS806-12 (2012), and Aly (2005) have had much higher errors than other models. The models proposed in this research have shown the lowest error compared to other available models. The Kriging and MARS models have had the lowest error values. Among the previous models, those of Esfahani *et al*. (2013), Choi *et al*. (2012), and Rakhshanimehr *et al*. (2018) have had a relatively better performance.

Fig. 4 shows box plots of the ratio of the bond strength predicted by different models to that found from experiments. As shown, in all proposed models, the mean of the data is lying next to ratio 1 which means the proposed soft computing models have had precise estimations of the experimental bond strength. The short length of the box plot in the proposed models means greater certainty and high

level of agreement in their predicted results. The Kriging and MARS models have, respectively, had the highest certainty. The length of the box plot in CAN/CSAS6-14 (2014) and CAN/CSA S806-12 (2012) models is higher than others showing great dispersed and scattered data in them. The first quartiles for CAN/CSAS6-14 (2014), CAN/CSAS806-12 (2012), and ACI440.1R-15 (2015) models are located higher than ratio 1, which means their estimations have been much higher than the experimental values. These design recommendations provide an unconservative prediction and considerably overestimate the bond strength of spliced GFRP bars for more than 75% of the specimens. Among previous researchers, Choi *et al*. (2012) have estimated the bond strength more accurately; however, their estimation has been more than the experimental value. Models presented by the JSCE (1997), Aly (2005), and Esfahani *et al*. (2013) have been quite conservative because their box plots of predicted to experimental bond strength ratio are below 1; that of Rakhshanimehr *et al*. (2018) also can be considered as relatively conservative. Although the proposed models are more complicated than previous ones, they have been able to significantly improve the certainty and prediction accuracy of the bond strength between GFRP bars and concrete in spliced concrete beams. This minor disadvantage can easily be defeated using the computer tool. It is worth noting that the bond strength may decrease over a long time (Bazli *et al*. 2017). The bond degradation of GFRP bars under various environmental conditions can be considered using an environmental reduction factor (ACI 440.1R-15 2015).

6. Conclusions

In this paper, a database of RC beam specimens with spliced GFRP bars in the splitting failure mode has been collected and used to find the GFRP bar-concrete bond strength. The concrete compressive strength, bar diameter, concrete cover, splice length, bar elasticity modulus, transverse reinforcement, and surface properties of GFRP bars have been considered as the main and basic parameters affecting the bond strength. To guarantee the generalization ability of the proposed models, training and testing data have been considered based on the ten-fold cross-validation technique. This paper has used such soft computing models as MARS, Kriging, and M5 to estimate the bond strength. Since regularization parameters highly affect the fitting of the models, these parameters have been so optimized in the proposed models to maximize the convergence coefficient of the training data and improve the accuracy and efficiency of the mentioned models. This optimization has been done with the GA and implemented in the MATLAB Software. The proposed new models intelligently find appropriate regularization parameters for the best model fitting. Results have shown that proposed models have significantly increased the prediction accuracy compared to previous models. The proposed MARS, Kriging, and M5 models have improved the convergence coefficient by approximately 65, 63 and 49%, respectively, compared to the best previous model. Regarding the statistical indices, MARS has had the least error in RMSE; Kriging stands next. Regarding AAE and MAE, Kriging has performed the best followed by the MARS. Most previous models have estimated the bond strength much more or much less than the test values, but the models proposed in this paper have predicted it more accurately with a lower standard deviation. A comparison of the box plot of the ratio of the predicted to experimental bond strengths has shown that Kriging and MARS have had much more accurate estimates than other models. It is worth noting that although the proposed models are more complicated, since they have considerably improved the bond strength predictions and access to computer tools is also easy, using them to find accurate and reliable results is justifiable. For design purposes, an environmental reduction factor can be considered to account for the bond degradation of GFRP bars under various environmental conditions.

References

Achillides, Z. (1998), "Bond behavior of FRP bars in concrete", Ph.D. Dissertation, Department of Civil and Structural Engineering, University of Sheffield.

Achillides, Z. and Pilakoutas, K. (2004), "Bond behavior of fiber reinforced polymer bars under direct pullout conditions", *J. Compos. Constr.*, ASCE, **8**(2), 173-181. https://doi.org/10.1061/(ASCE)1090-0268(2004)8:2(173).

ACI Committee 440.1R-03 (2003), Guide for the Design and Construction of Concrete Reinforced with FRP Bars, American Concrete Institute, Farmington Hills, Michigan.

ACI Committee 440.1R-06 (2006), Guide for the Design and Construction of Structural Concrete Reinforced with FRP Bars, American Concrete Institute, Farmington Hills, Michigan.

ACI Committee 440.1R-15 (2015), Guide for the Design and Construction of Structural Concrete Reinforced with FRP Bars, American Concrete Institute, Farmington Hills, Michigan.

Ahmad, S., Pilakoutas, K., Rafi, M.M. and Zaman, Q.U. (2018), "Bond strength prediction of steel bars in low strength concrete by using ANN", *Comput. Concrete*, **22**(2), 249-259. https://doi.org/10.12989/cac.2018.22.2.249.

Al-Mudhafar, W.J. (2019), "Bayesian kriging for reproducing reservoir heterogeneity in a tidal depositional environment of a sandstone formation", *J. Appl. Geophys.*, **160**, 84-102. https://doi.org/10.1016/j.jappgeo.2018.11.007.

Aly, R. (2005), "Experimental and analytical studies on bond behavior of tensile lap spliced FRP reinforcing bars in concrete", Ph.D. Dissertation, Department of Civil Engineering, University of Sherbrook, Sherbrook.

Ashrafi, H., Bazli, M. and Vatani Oskouei, A. (2017), "Enhancement of bond characteristics of ribbed-surface GFRP bars with concrete by using carbon fiber mat anchorage", *Constr. Build. Mater.*, **134**, 507-519. https://doi.org/10.1016/j.conbuildmat.2016.12.083.

Asteris, P.G., Ashrafian, A. and Rezaie-Balf, M. (2019), "Prediction of the compressive strength of self-compacting concrete using surrogate models", *Comput. Concrete*, **24**(2), 137-150. https://doi.org/10.12989/cac.2019.24.2.137.

Baena, M., Torres, L., Turon, A. and Barris, C. (2009), "Experimental study of bond behavior between concrete and FRP bars using a pull-out test", *Compos. Part B*, **40**(8), 784-797. https://doi.org/10.1016/j.compositesb.2009.07.003.

Bazli, M., Ashrafi, H. and Vatani Oskouei, A. (2017), "Experiments and probabilistic models of bond strength between GFRP bar and different types of concrete under aggressive environments", *Constr. Build. Mater.*, **148**, 429-443.

https://doi.org/10.1016/j.conbuildmat.2017.05.046.
Behnood, A., Olek, J. and Glinicki, M.A. (2015), "Predicting modulus elasticity of recycled aggregate concrete using M5 model tree algorithm", *Constr. Build. Mater.*, **94**, 137-147. https://doi.org/10.1016/j.conbuildmat.2015.06.055.
CAN/CSA S6-14 (2014), Canadian Highway Bridge Design Code, Canadian Standards Association, Ontario, Canada.
CAN/CSA S806-12 (2012), Design and Construction of Building Components with Fiber Reinforced Polymers, Canadian Standards Association, Ontario, Canada.
Chaallal, O. and Benmokrane, B. (1993), "Pullout and bond of glass fibre rods embedded in concrete and cement grout", *Mater. Struct.*, **26**(3), 167-175. https://doi.org/10.1007/BF02472934.
Choi, D.U., Chun, S.C. and Ha, S.S. (2012), "Bond strength of glass fiber-reinforced polymer bars in unconfined concrete", *Eng. Struct.*, **34**, 303-313. https://doi.org/10.1016/j.engstruct.2011.08.033.
Choi, Y.C., Bae, B.I., Cho, K.H. and Choi, H.K. (2014), "Experimental study on the performance of tensile lap-spliced GFRP rebars in concrete beam", *Mag. Concrete Res.*, **66**(24), 1250-1262. https://doi.org/10.1680/macr.14.00111.
Conoscenti, C., Rotigliano, E., Cama, M., Caraballo-Arias, N.A., Lombardo, L. and Agnesi, V. (2016), "Exploring the effect of absence selection on landslide susceptibility models: a case study in Sicily, Italy", *Geomorphology*, **261**, 222-235. https://doi.org/10.1016/j.geomorph.2016.03.006.
Ehsani, M.R., Saadatmanesh, H. and Tao, S. (1993), "Bond of GFRP rebars to ordinary-strength concrete", *ACI Int. Symp. on Non-Metallic Continuous Reinforcement*, Vancouver, Canada.
Ehsani, M.R., Saadetmanesh, H. and Tao, S. (1996), "Design recommendation for bond of GFRP bars to concrete", *J. Struct. Eng.*, ASCE, **122**(3), 247-254.
Esfahani, M.R., Rakhshanimehr, M. and Mousavi, S.R. (2013), "Bond strength of lap-spliced GFRP bars in concrete beams", *J. Compos. Constr.*, ASCE, **17**(3), 314-323. https://doi.org/10.1061/(ASCE)CC.1943-5614.0000359.
Faza, S.S. and GangaRao, H.V.S. (1990), "Bending and bond behaviour of concrete beams reinforced with plastic rebars", Transportation Research Record, No. 1290, 185-193.
Friedman, J.H. (1991), "Multivariate adaptive regression splines", *Ann. Statist.*, **19**(1), 1-67.
Golafshani, E.M., Rahai, A. and Hosseini Kebria, S.S. (2014), "Prediction of the bond strength of ribbed steel bars in concrete based on genetic programming", *Comput. Concrete*, **14**(3), 327-345. https://doi.org/10.12989/cac.2014.14.3.327 327.
Golafshani, E.M., Rahai, A. and Sebt, M.H. (2015), "Artificial neural network and genetic programming for predicting the bond strength of GFRP bars in concrete", *Mater. Struct.*, **48**(5), 1581-1602. https://doi.org/10.1617/s11527-014-0256-0.
Güneyisi, E.M., Mermerdaş, K. and Gültekin, A. (2016), "Evaluation and modeling of ultimate bond strength of corroded reinforcement in reinforced concrete elements", *Mater. Struct.*, **49**(8), 3195-3215. https://doi.org/10.1617/s11527-015-0713-4.
Hao, Q.D., Wang, B. and Ou, J.P. (2006), "Fiber reinforced polymer rebar's application to civil engineering", *Concrete*, **9**, 38-40.
Harajli, M. and Abouniaj, M. (2010), "Bond performance of GFRP bars in tension: experimental evaluation and assessment of ACI 440 guidelines", *J. Compos. Constr.*, ASCE, **14**(6), 659-668. https://doi.org/10.1061/(ASCE)CC.1943-5614.0000139.
Hossain, K.M.A., Ametrano, D. and Lachemi, M. (2017), "Bond strength of GFRP bars in ultra-high strength concrete using RILEM beam tests", *J. Build. Eng.*, **10**, 69-79. https://doi.org/10.1016/j.jobe.2017.02.005.
Japan Society of Civil Engineers, JSCE (1997), Recommendation for Design and Construction of Concrete Structures Using Continuous Fiber Reinforcing Materials, Tokyo, Japan.
Jekabsons, G. (2010a), "ARESLab: Adaptive Regression Splines toolbox for MATLAB/Octave", Institute of Applied Computer Systems, Riga Technical University, Latvia.
Jekabsons, G. (2010b), "M5PrimeLab: M5' Regression Tree, Model Tree, and tree ensemble toolbox for MATLAB/Octave", Institute of Applied Computer Systems, Riga Technical University, Latvia.
Kanakubo, T., Yonemaru, K., Fukuyama, H., Fujisawa, M. and Sonobe, Y. (1993), "Bond performance of concrete members reinforced with FRP bars", *International Symposium: Fiber-Reinforced Plastic Reinforcement for Concrete Structues*, SP138, ACI Proceedings, 767-788.
Koroglu, M.A. (2018), "Artificial neural network for predicting the flexural bond strength of FRP bars in concrete", *Sci. Eng. Compos. Mater.*, **26**(1), 12-29. https://doi.org/10.1515/secm-2017-0155.
Kotynia, R., Szczech, D. and Kaszubska, M. (2017), "Bond behavior of GRFP bars to concrete in beam test", *Procedia Eng.*, **193**, 401-408. https://doi.org/10.1016/j.proeng.2017.06.230.
Krige, D. (1951), "A stitistical approach to some basic mine valuation problems on the witwatersrand", *J. South. Afr. Inst. Min. Metal.*, **52**, 119-139.
Lee, J.Y., Yi, C.K. and Cheong, Y.G. (2009), "Experimental study on the FRP-concrete bond behavior under repeated loadings", *Mech. Compos. Mater.*, **45**(6), 609-618. https://doi.org/10.1007/s11029-010-9117-2.
Li, C. and Pan, Q. (2019), "Adaptive optimization methodology based on Kriging modeling and a trust region method" *Chinese J. Aeronaut.*, **32**(2), 281-295. https://doi.org/10.1016/j.cja.2018.11.012.
Lin, H., Zhao, Y., Feng, P., Ye, H., Ozbolt, J., Jiang, C. and Yang, J.Q. (2019), "State-of-the-art review on the bond properties of corroded reinforcing steel bar", *Constr. Build. Mater.*, **213**, 216-233. https://doi.org/10.1016/j.conbuildmat.2019.04.077.
Lophaven, S.N., Nielsen, H.B. and Sndergaard, J. (2002), DACE-a MATLAB Kriging Toolbox, Ver. 2.0, IMM, Kongens Lyngby, Denmark.
Makitani, E., Irisawa, I. and Nishiura, N. (1993), "Investigation of bond in concrete member with fibre reinforced plastic bars", *Fibre-Reinforced-Plastic Reinforcement for Concrete Structures International Symposium*, ACI SP138-20, 315-331.
Mallipeddi, R. and Lee, M. (2015), "An evolving surrogate model-based differential evolution algorithm", *Appl. Soft Comput.*, **34**, 770-787. https://doi.org/10.1016/j.asoc.2015.06.010.
Malvar, L.J. (1994), "Bond stress-slip characteristics of FRP rebars", Report TR- 2013-SHR, Naval Facilities Eng. Service Center, Port Hueneme, California.
Mansouri, I., Ozbakkaloglu, T., Kisi, O. and Xie, T. (2016), "Predicting behavior of FRP-confined concrete using neuro fuzzy, neural network, multivariate adaptive regression splines and M5 model tree techniques", *Mater. Struct.*, **49**(10), 4319-4334. https://doi.org/10.1617/s11527-015-0790-4.
Matheron, G. (1970), *Random Functions and their Applications in Geology*, Springer, Plenum, New York.
Maurel, O., Dekoster, M. and Buyle-Bodin, F. (2005), "Relation between total degradation of steel concrete bond and degree of corrosion of RC beams experimental and computational studies", *Comput. Concrete*, **2**(1), 1-18. https://doi.org/10.12989/cac.2005.2.1.001.
Moodi, Y., Farahi Shahri, S. and Mousavi, S.R. (2017), "Providing a model for estimating the compressive strength of square and rectangular columns confined with a variety of fibre-reinforced polymer sheets", *J. Reinf. Plast. Compos.*, **36**(21), 1602-1612. https://doi.org/10.1177/0731684417720837.
Mosley, C.P., Tureyen, A.K. and Frosch, R.J. (2008), "Bond strength of nonmetallic reinforcing bars", *ACI Struct. J.*, **105**(5),

634-642.

Nanni, A., Al-Zaharani, M., Al-Dulaijan, S., Bakis, C. and Boothby, I. (1995), "Bond of FRP reinforcement to concrete-experimental results", *Non-metallic (FRP) Reinforcement for Concrete Struct., Proceedings of the Second Int. RILEM Symposium*, CRC Press.

Nguyen, H., Bui, X.N., Tran, Q.H. and Mai, N.L. (2019), "A new soft computing model for estimating and controlling blast-produced ground vibration based on Hierarchical K-means clustering and Cubist algorithms", *Appl. Soft Comput.*, **77**, 376-386. https://doi.org/10.1016/j.asoc.2019.01.042.

Okelo, R. and Yuan, R.L. (2005), "Bond strength of fiber reinforced polymer reinforcement bars in normal strength concrete", *J. Compos. Constr.*, ASCE, **9**(3), 203-213. https://doi.org/10.1061/(ASCE)1090-0268(2005)9:3(203).

Orangun, C.O., Jirsa, J.O. and Breen, J.E. (1977), "Reevaluation of test data on development length and splices", *ACI J. Proc.*, **74**(3), 114-122.

Park, J.S., Lim, A.R., Kim, J. and Lee, J.Y. (2016), "Bond performance of fiber-reinforced polymer rebars in different casting positions", *Polym. Compos.*, **37**(7), 2098-2108. https://doi.org/10.1002/pc.23388.

Pay, A.C., Canbay, E. and Frosch, R.J. (2014), "Bond strength of spliced fiber-reinforced polymer reinforcement", *ACI Struct. J.*, **111**(2), 257-266.

Pleimann, L.G. (1987), "Tension and bond pull-out tests of deformed fibreglass rods", Final Report for Marshall-Vega Corporation, Marshall, Arkansas, Civil Engineering Department, University of Arkansas, Fayetteville, 5-11.

Quinlan, J.R. (1992), "Learning with continuous classes", *Proceedings of Australian Joint Conference on Artificial Intelligence*, World Scientific Press, Singapore.

Rakhshanimehr, M., Mousavi, S.R., Esfahani, M.R. and Farahi Shahri, S. (2018), "Establishment and experimental validation of an updated predictive equation for the development and lap-spliced length of GFRP bars in concrete", *Mater. Struct.*, **51**(15). https://doi.org/10.1617/s11527-018-1137-8.

Rezaei, A. (2017), "Effect of transverse reinforcement on the bond strength of spliced GFRP bars in concrete beams", Master Dissertation, University of Sistan and Baluchestan, Zahedan, Iran. (in Persian)

Sacks, J., Welch, W.J., Mitchell, T.J. and Wynn, H.P. (1989), "Design and analysis of computer experiments", *Stat. Sci.*, **4**(4), 409-435.

Saleh, N., Ashour, A., Lam, D. and Sheehan, T. (2019), "Experimental investigation of bond behaviour of two common GFRP bar types in high-strength concrete", *Constr. Build. Mater.*, **201**, 610-622. https://doi.org/10.1016/j.conbuildmat.2018.12.175.

Shirkhani, A., Davarnia, D. and Farahmand Azar, B. (2019), "Prediction of bond strength between concrete and rebar under corrosion using ANN", *Comput. Concrete*, **23**(4), 273-279. https://doi.org/10.12989/cac.2019.23.4.273.

Tepfers, R. (1982), "Tensile lap splices with confining reinforcement", *Contribution to the Int. Conference on Bond in Concrete*, Paisley, Scotland, 318-330.

Tighiouart, B., Benmokrane, B. and Gao, D. (1998), "Investigation of bond in concrete member with fibre reinforced polymer (FRP) bars", *Constr. Build. Mater.*, **12**(8), 453-462. https://doi.org/10.1016 /S0950-0618(98)00027-0.

Tighiouart, B., Benmokrane, B. and Mukhopadhyaya, P. (1999), "Bond strength of glass FRP rebars splices in beams under static loading", *Constr. Build. Mater.*, **13**(7), 383-392. https://doi.org/10.1016/S0950-0618(99)00037-9.

Turk, K., Caliskan, S. and Yildirim, M.S. (2005), "Influence of loading condition and reinforcement size on the concrete/reinforcement bond strength", *Struct. Eng. Mech.*, **19**(3), 337-346. https://doi.org/10.12989/sem.2005.19.3.337.

Wambeke, B. and Shield, C. (2006), "Development length of glass fiber-reinforced polymer bars in concrete", *ACI Struct. J.*, **103**(1), 11-17.

Wang, X. and Liu, X. (2004), "Bond strength modeling for corroded reinforcement in reinforced concrete", *Struct. Eng. Mech.*, **17**(6), 863-878. https://doi.org/10.12989/sem.2004.17.6.863.

Wang, Y. and Witten, I.H. (1997), "Induction of model trees for predicting continuous classes", *Proceedings of the Poster Papers of the European Conference on Machine Learning*, University of Economics, Prague, Czech Republic.

Williams, K.T. and Gomez, J.D. (2016), "Predicting future monthly residential energy consumption using building characteristics and climate data: a statistical learning approach", *Energy Build.*, **128**, 1-11. https://doi.org/10.1016/j.enbuild.2016.06.076.

Xue, W., Zheng, Q., Yang, Y. and Fang, Z. (2014), "Bond behavior of sand-coated deformed glass fiber reinforced polymer rebars", *J. Reinf. Plast. Compos.*, **33**(10), 895-910. https://doi.org/10.1177/073168441352 0263.

Yao, L., Zhang, L., Zhang, L. and Li, X. (2015), "Prediction of initiation time of corrosion in RC using meshless methods", *Comput. Concrete*, **16**(5), 669-682. https://doi.org/10.12989/cac.2015.16.5.669.

Zemour, N., Asadian, A., Ahmed, E.H., Khayat, K.H. and Benmokrane, B. (2018), "Experimental study on the bond behavior of GFRP bars in normal and self-consolidating concrete", *Constr. Build. Mater.*, **189**, 869-881. https://doi.org/10.1016/j.conbuildmat.2018.09.045.

Zhou, J., Chen, X. and Chen, S. (2012), "Effect of different environments on bond strength of glass fiber-reinforced polymer and steel reinforcing bars", *KSCE J. Civil Eng.*, **16**(6), 994-1002. https://doi.org/10.1007/s12205-012-1462-3.

HK